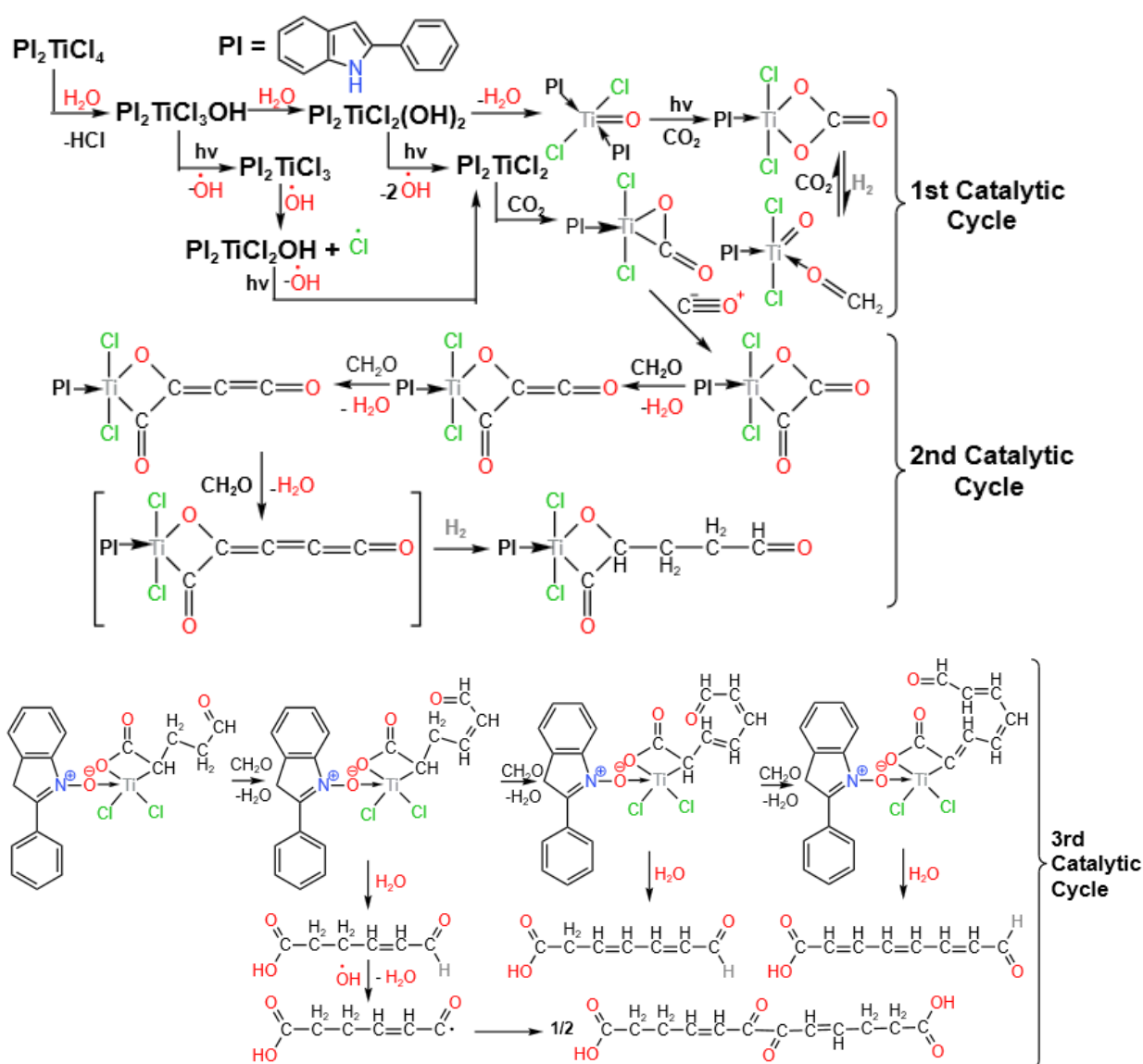


# C<sub>6</sub> to C<sub>17</sub> Organic Products from Artificial Photosynthesis Catalyzed by 2-Phenyl Indole (PI) Titanium Tetrachloride Complex (PI)<sub>2</sub>TiCl<sub>4</sub>. The Synergism of Hydroxyl Radicals.

Gregory G. Arzoumanidis<sup>\*1</sup> and Michail Paraskevas<sup>2</sup>

1. Oakwood Consulting, Inc. Naperville, IL 60540, USA. E-mail: arzoumandis@gmail.com
2. Quangdong Technion Israel Institute of Technology, Jinping, Shantou, Quangdong 515063, P. R. China



**Abstract.** The newly discovered artificial photosynthesis process catalyzed by 2-phenyl indole (PI) and  $TiCl_4$  complexes activated by visible light, produces long-chain oxygenated hydrocarbons up to C<sub>17</sub>. This process begins with the formation of  $\alpha$ -carboxylic acid- $\omega$ -aldehyde compounds (C<sub>6</sub> to C<sub>9</sub>), arising from a cascade of autocatalytic organotitanium complexes derived from  $(PI)_2TiCl_4$ . These complexes are formed via hydrolysis by ambient air

humidity and the direct atmospheric capture (DAC) of CO<sub>2</sub>. Carbon chain growth utilizes system-generated formaldehyde as a feedstock. The initial C<sub>6</sub> to C<sub>9</sub> compounds can further couple to C<sub>12</sub> to C<sub>17</sub> derivatives through a radical mechanism initiated by hydroxyl radicals. A proposed mechanism explores the synergistic interaction between organotitanium catalysis and hydroxyl radicals. This development represents the only known heterogeneous catalytic system that autonomously captures CO<sub>2</sub> and humidity from the atmosphere to subsequently produce long-chain oxygenated hydrocarbons using solar energy.

**Keywords:** Artificial Photosynthesis, Photocatalysis, Organotitanium Complexes, CO<sub>2</sub> Capture, Hydroxyl Radicals

## 1. Introduction

Most artificial photosynthesis (AP) systems, including those at the forefront of research, focus on water splitting for hydrogen production or reducing CO<sub>2</sub> to basic hydrocarbons (C<sub>1</sub>-C<sub>3</sub>). The ability to synthesize long-chain compounds (up to C<sub>17</sub>) offers a transformative opportunity to produce higher-value chemicals, advancing AP technology scalability.

The newly developed TiCl<sub>4</sub>/2-phenylindole (PI) photocatalytic system uses visible light to convert atmospheric CO<sub>2</sub> and H<sub>2</sub>O into multi-carbon oxygenated hydrocarbons<sup>1</sup>. This breakthrough integrates Direct Air Capture (DAC) of CO<sub>2</sub> with conversion, addressing critical challenges in climate change, energy sustainability, and resource efficiency.

The mechanism involves forming photoactive Ti<sup>4+</sup>-OH bonds through the hydrolysis of Ti<sup>4+</sup>-Cl bonds by ambient air humidity. Upon exposure to light and air, these Ti<sup>4+</sup>-OH bonds release hydroxyl radicals, facilitating the reduction of the titanium center (Ti<sup>4+</sup> → Ti<sup>3+</sup>/Ti<sup>2+</sup>). The reduced titanium species, with increased electron density, effectively capture atmospheric CO<sub>2</sub>, initiating a spontaneous and intricate reduction process that produces long-chain oxygenated hydrocarbons. This solar-driven, autonomous production distinguishes the system from conventional AP methods.

Traditional AP approaches primarily target water splitting and CO<sub>2</sub> reduction to small hydrocarbons (C<sub>1</sub>-C<sub>3</sub>) using metal oxide catalysts. These methods often require high CO<sub>2</sub> concentrations and separate processes, achieving limited success. In contrast, the novel organotitanium-based system integrates water splitting and CO<sub>2</sub> reduction into a single, continuous process, producing oxygenated organics directly from ambient CO<sub>2</sub> (~0.04%). This capability to convert trace amounts of CO<sub>2</sub> into valuable materials represents a significant leap in AP technology.

A crucial feature of this system is the photocatalytic generation of hydroxyl radicals, released from Ti<sup>4+</sup>-OH, Ti<sup>3+</sup>-OH, and Ti<sup>2+</sup>-OH bonds. With a redox potential of 2.8 V (second only to fluorine), hydroxyl radicals are highly reactive, yet transient species that drive the organotitanium catalytic process. While TiO<sub>2</sub> photocatalysis is known to produce hydroxyl radicals, their synergistic role in facilitating complex reaction cascades in this system is unprecedented.

Although hydroxyl radicals typically exist on the nanosecond scale, they can persist for up to 600 seconds in aqueous environments, enabling diverse redox reactions. These include dimerization to form H<sub>2</sub>O<sub>2</sub>, oxidation of Ti=O bonds to peroxo-titanium species (Ti-O-O), oxidation of PI ligands to N-O functionalities, conversion of CO<sub>2</sub> to HCOOH, and condensation or radical coupling involving formaldehyde-derived intermediates.

The autonomous, multi-step nature of this system—driven by hydroxyl radical-mediated pathways—highlights its efficiency and versatility. Understanding these transformations is essential for optimizing or tailoring the system for specific goals, such as oxygen production via hydroxyl radical dimerization, where pH significantly influences outcomes.

This system's ability to sustain multiple valuable reactions in a continuous process, especially DAC and CO<sub>2</sub> reduction, underscores its transformative potential. Further investigation into its mechanism could unlock even greater industrial and environmental applications.

## 2. Results and Discussion

### 2.1 Focus

Our research explores the synthesis of oxygenated hydrocarbon products with linear chains up to C<sub>17</sub> using an organotitanium photocatalytic system. This breakthrough enables the direct conversion of atmospheric carbon into complex, long-chain organic molecules, advancing green chemistry and renewable energy goals. The visible-light-activated organotitanium complexes exhibit self-organizing behavior, forming autocatalytic reaction networks. These networks drive three self-sustaining cycles, where reaction products catalyze subsequent reactions, showcasing an innovative approach to sustainable molecular assembly.

### 2.2 First Catalytic Cycle

In the first photocatalytic cycle, the (PI)<sub>2</sub>TiCl<sub>4</sub> complex serves as the essential "starter" catalyst, initiating a self-organized cascade. This complex interacts autonomously in the solid state with environmental inputs—visible light, H<sub>2</sub>O, and CO<sub>2</sub>—evolving into a sophisticated, multi-component photocatalytic system. Similar photocatalytic behavior has been observed in titanium click chemistry studies<sup>8</sup>.

The process begins with hydrolysis of (PI)<sub>2</sub>TiCl<sub>4</sub> by atmospheric moisture, forming intermediate complex **1**, which converts to complex **2** (see *Figure 1*). Under visible light, complex **1** reacts with CO<sub>2</sub>, forming organotitanium carbonate complex **10** (illustrated in *Figure 2*), while complex **2** releases hydroxyl radicals, generating Ti<sup>+2</sup> complex **3**. Complexes **1** and **3** capture atmospheric CO<sub>2</sub> (0.04%), a significant advance for climate change mitigation research.

Complex **4** coordinates with system-generated CO, replacing a PI ligand to form complex **8**. This coordination facilitates CO insertion into the Ti-C bond, yielding the unique titanium α-ketocarboxylate complex **9**. The four-membered Ti-O-C-C titanaoxetane ring structure, previously observed<sup>9</sup> in rhodium, silver, and other metals, appears for the first time in titanium chemistry as a ketocarboxylate ring.

Alternatively, complex **4** undergoes hydrolysis to form complex **5**, which, upon irradiation, releases hydroxyl radicals and transforms into complex **6**. This complex then rearranges into formaldehyde coordination complex **7**, by reacting with the newly released hydroxyl radicals.

The carbonate complex **10** (*Figure 2*), formed from activated complex **1** and captured atmospheric CO<sub>2</sub>, can generate formaldehyde (complex **12**) and/or methanol (complex **13**) through a hydrogenation mechanism. Hydrogen is produced internally via photocatalytic water splitting<sup>1</sup>. The continuous catalytic cycle shown in *Figure 2*, incorporating DAC of CO<sub>2</sub>, provides a sustainable

source of formaldehyde and methanol as valuable feedstocks.

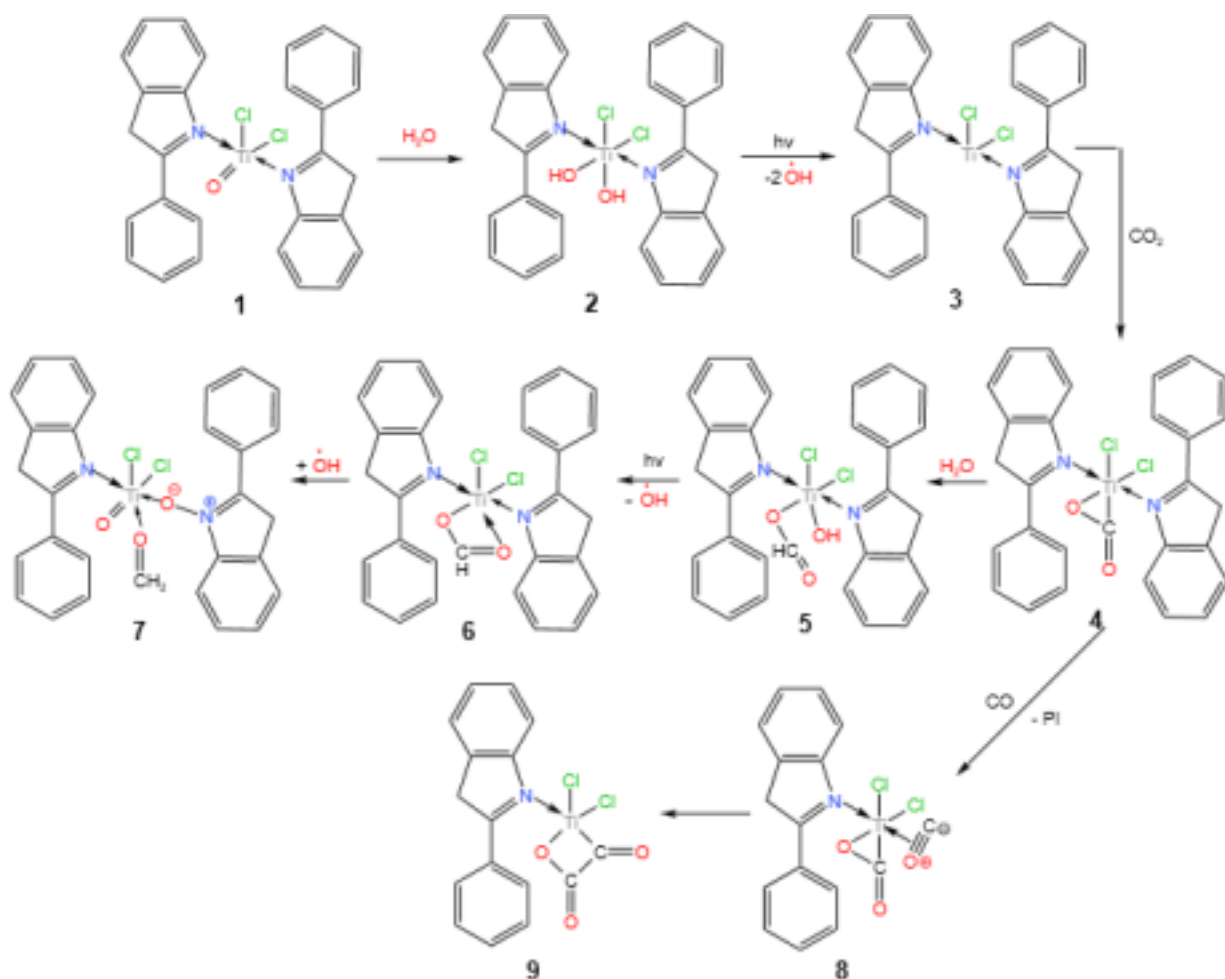


Figure 1. Initiation of the photocatalytic process based on  $(PI)_2TiCl_4$ .

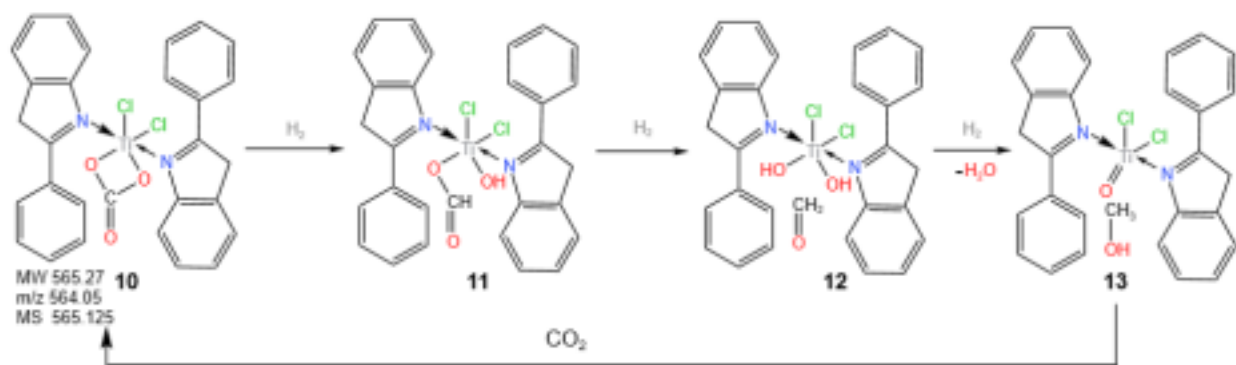


Figure 2. Hydrogenation of carbonate complex 10 yielding formaldehyde (complex 12) and/or methanol (complex 13).

### 2.3. Second Catalytic Cycle

The THF-coordinated analog of complex 9, identified as complex 14 (Figure 3) in MALDI-TOF analysis, initiates a new cycle in the cascade process, aiding the formation of long-chain organics. It uses formaldehyde as a building block, leading to the formation of complexes 15, 16, and 17. The THF coordination in complexes 14–17 is specific to the

experimental conditions, as these were conducted in THF. In the absence of THF, complex **9** is expected to directly coordinate with formaldehyde.

The  $\alpha$ -ketocarboxylate complex **14** undergoes a photocatalytic transformation to form ketene complex **15** and cumulene derivative **16** through a condensation with formaldehyde. The reaction involves dehydration via  $\text{H}_2\text{O}$  elimination, followed by hydrogenation to yield complex **17**. While not detected by MALDI-TOF, it seems that a third condensation step occurs, likely contributing to the partially hydrogenated product. Complex **17**, with four carbon atoms on the pendant chain, leads to the PI oxygenated analog (complex **21**, Figure 6), which is crucial in the third and final catalytic cycle.

Titanium in complex **14** is highly electrophilic due to the electron-withdrawing chloride ligands and the carbonyl moieties of the titanaoxetane ring. This allows formaldehyde, with its nucleophilic oxygen, to react readily with the titanium center, forming complex **18** (Figure 4). The second catalytic cycle begins with complex **14**, which initiates a novel formaldehyde condensation process, driving the formation of long-chain organic molecules through a series of orchestrated steps outlined below:

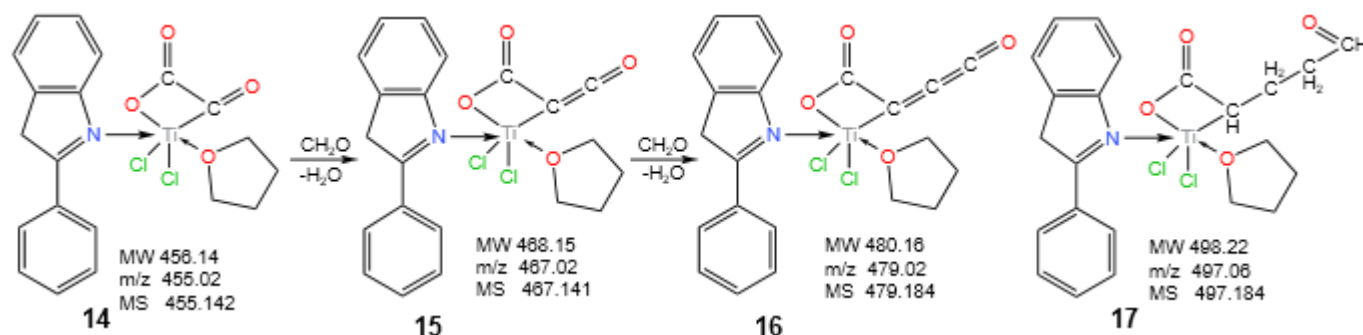


**Figure 3.** Photocatalytic conversion of the  $\alpha$ -ketocarboxylate complex **14** results in ketene **15** and cumulene derivative **16** via an apparent formaldehyde condensation with a keto group, accompanied by  $\text{H}_2\text{O}$  elimination. The hydrogenated complex **17** likely originates from a related intermediate, featuring a pendant carbon chain with four carbon atoms

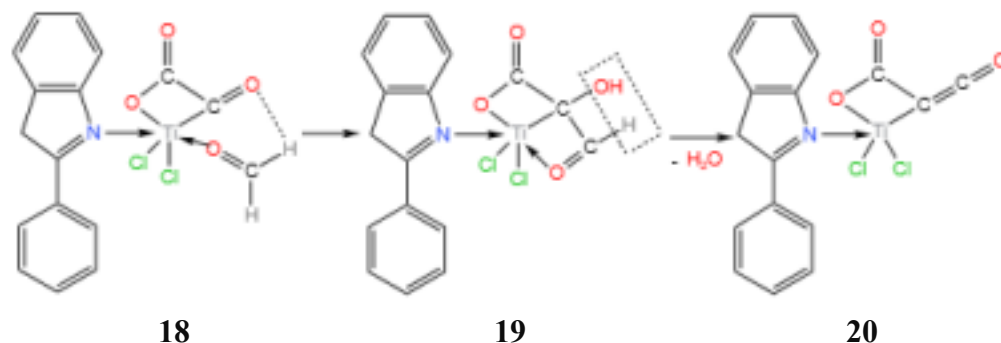


**Figure 4.** Aldol-type condensation of formaldehyde coordinated to titanium, leading to dehydration and formation of ketene complex **20**.

- 1. Formation of Ketene:** An Aldol condensation occurs between formaldehyde and the carbonyl group of complex **14**, facilitated by the coordination of formaldehyde to titanium, as shown in Figure 4.
- 2. Repeating Reactions:** The Aldol condensation proceeds iteratively, forming complex **16** with a cumulene side chain. While formaldehyde could theoretically react further with complex **16** to produce a compound containing four consecutive double bonds, such a structure would be intrinsically unstable. Nonetheless, evidence for the transient existence

of such intermediate is supported by the detection of hydrogenated complex **17**, characterized by a side chain of four carbon atoms, terminating in a reactive aldehyde group.

Again, the reaction sequence of the second cycle underscore the central role of complex **9** (or the analogous THF coordinated **14**) as the initiating catalyst and driver, achieving long-chain organic molecules production.

## 2.4. MALDI-TOF MS Data.

The structures of catalytic intermediates formed through the cascade transformations of the original  $(\text{PI})_2\text{TiCl}_4$  complex were primarily elucidated via MALDI-TOF MS (Matrix-Assisted Laser Desorption Ionization-Time of Flight Mass Spectrometry), which has proven highly effective in characterizing transition metal catalysts<sup>10,11</sup>. MALDI-TOF is particularly advantageous for identifying intact metal complexes. Besides MALDI-TOF, the detailed process of deciphering this dynamic chemical system's cascade sequence and verifying individual complexes and other products was supported by other key observations as well:

(a) Comparative reactivity analysis of similar organotitanium systems, including hydroxyl radical formation by a substituted ansa-titanocene dihydroxido complex under daylight irradiation<sup>2,3</sup> and the established ability of titanium oxo ( $\text{Ti}=\text{O}$ ) groups to convert to peroxo species ( $\text{Ti}-\text{O}-\text{O}-$ ) upon  $\text{H}_2\text{O}_2$  exposure; (b) Observations of ordered reaction sequences across multiple sub-cycles of the photosynthetic cascade, as illustrated in Figures 1 and 2; (c) Expected formation of trichloro- and dichloro-titanium PI complexes upon daylight-induced reduction of the titanium tetrachloride PI coordination compound<sup>12</sup>.

Complexes in *Figure 1*<sup>1</sup>, *Figure 2* and *Figure 3* are labeled with calculated molecular weights (MW) and expected  $m/z$  ratios, which reflect the natural isotopic distribution of the elements in each complex, along with the experimentally recorded MALDI-TOF MS data. The close match between calculated (MW,  $m/z$ ) values and the experimental MS data strongly support the structural identity of each complex.

*Figure 5* displays the MALDI-TOF spectrum in  $\text{CH}_2\text{Cl}_2$  for a  $(\text{PI})_2\text{TiCl}_4$  complex exposed to air and daylight over three weeks, highlighting mostly organic products. These products and their identities are discussed in detail. The relative concentrations of these materials are represented by the relative peak intensities in the MALDI-TOF spectrum, summarized in Table 1. The identification of each organotitanium catalytic intermediate was addressed in our previous publication<sup>1</sup>, which includes *Figure 5*.



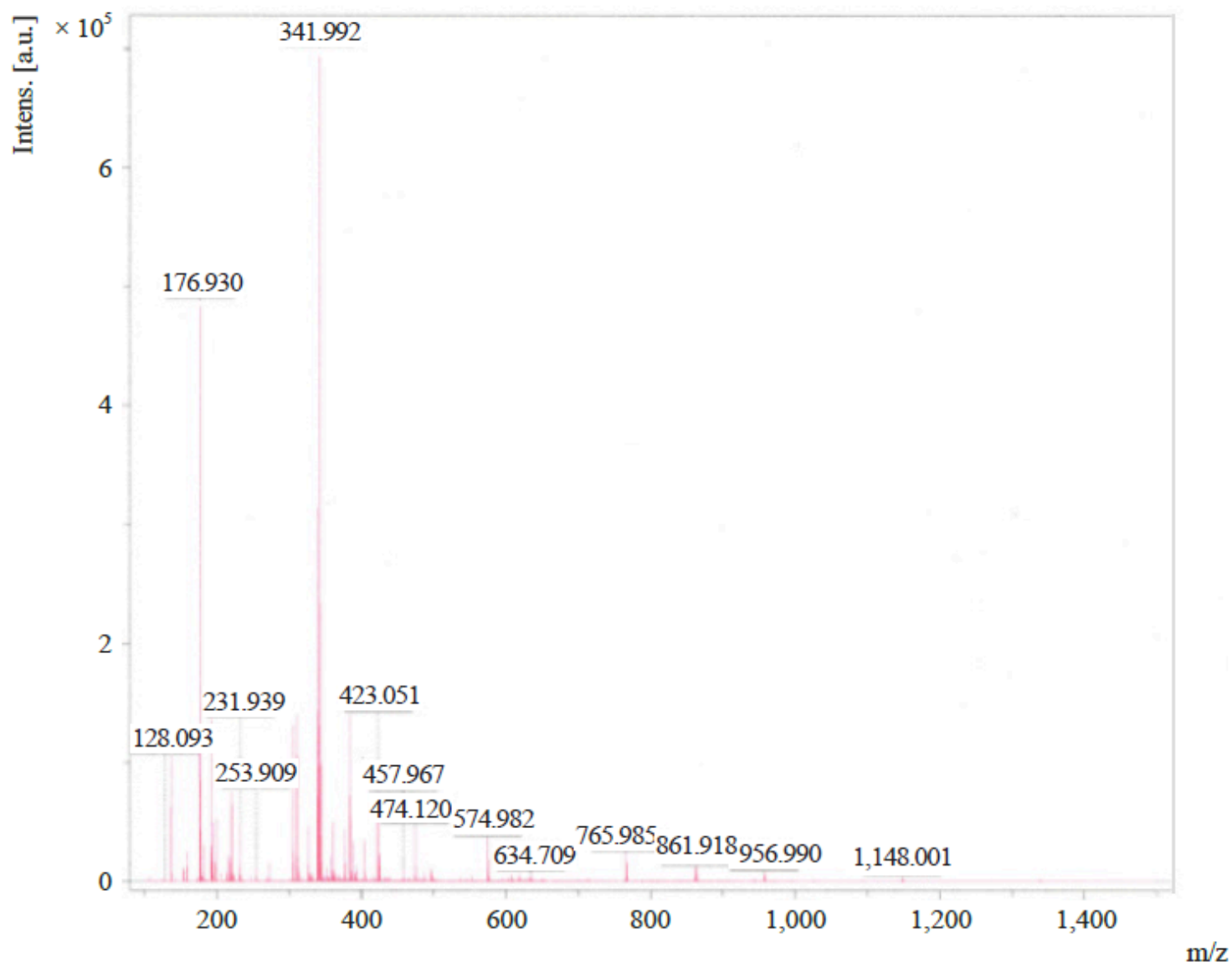


Figure 5. Maldi-Tof spectrum in  $\text{CH}_2\text{Cl}_2$  featuring organic products from artificial photosynthesis catalyzed by  $(\text{PI})_2\text{TiCl}_4$ .

Table 1. Intensities of MALDI-TOF recorded data from Figure 2.

Nu.	MS	Intensity	Nu.	MS	Intensity	Nu.	MS	Intensity
1	128.093	vw	11	272	w	21	423.051	w
2	140	m	12	306	m	22	457.947	w
3	152	vw	13	313.7	m	23	474.12	m
4	156	w	14	328	w	24	487	vw
5	176.950	s	15	341.992	vs	25	495	vw
6	193	m	16	358	w	26	574.982	w
7	199	w	17	378	w	27	634.982	vw
8	216	m	18	382	m	28	765.985	w
9	231.939	w	19	386	w	29	861.918	vw
10	253.909	vw	20	404	w	30	956.990	vw
						31	1148.001	vw

w=weak, vw=very weak, m=medium, s=strong, vs=very strong

## 2.5. Third Catalytic Cycle.

The cascade operation continues with a third cycle, as shown in *Figure 6*. It begins with the N-oxidation of the PI ligand in complex **17**, most likely facilitated by hydroxyl radicals, forming complex **21**. This new sequence introduces a unique formaldehyde condensation process involving the aldehyde group on the side chain of the organotitanium complexes. This leads to the consecutive formation of complexes **22**, **23**, and **24**, marking another step in the cascade transformation.

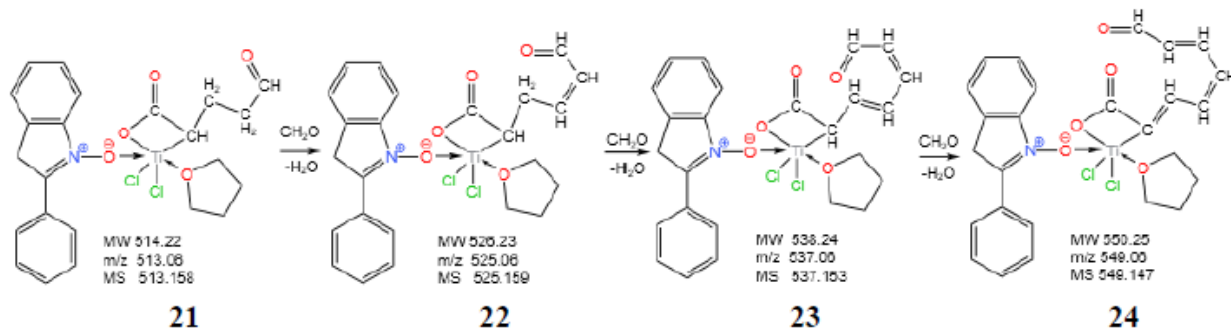


*Figure 6. Third catalytic cycle. New-type condensation of formaldehyde with the aldehyde group of the side chain on organotitanium complex **21**. Consecutive carbon addition and double-bond creation on the side chain, from complex **21** to complex **24**.*

A breakdown of the second sub-cycle highlights the following key steps:

- 1. N-Oxidation:** Complex **17** undergoes N-oxidation by hydroxyl radicals to form complex **21**, initiating the third sub-cycle.
- 2. Condensation with Formaldehyde:** Complex **21** reacts with formaldehyde, forming complex **22**, which undergoes two further condensations to yield complexes **23** and **24**.
- 3. Carbon Chain Growth:** Each condensation extends the carbon chain, adding a unit and creating conjugated double bonds. The process halts when the double bond reaches the titanaoxetane ring in complex **24**.
- 4. Formation of Unsaturated  $\alpha$ -Carboxylic Acids- $\omega$ -Aldehydes:** Complexes **22**, **23**, and **24** serve as precursors to C<sub>6</sub>, C<sub>7</sub>, and C<sub>8</sub> unsaturated  $\alpha$ -carboxylic acids- $\omega$ -aldehydes, respectively, see below. These compounds are produced autonomously by the system from their respective organotitanium complexes, by an apparent hydrolysis.
- 5. Potential for Further Growth:** The linear carbon chains can further grow up to C<sub>17</sub>, by a radical coupling process initiated by hydroxyl radicals. Additional details are provided later in the text.

The third cycle reaction sequence illustrates a novel formaldehyde condensation mechanism, enabling complex organotitanium structures to autonomously generate unsaturated  $\alpha,\omega$ -carboxylic acids-aldehydes. This process exhibits significant potential for additional carbon chain growth and radical coupling reactions. These advancements further underline the



system's ability to construct intricate organic frameworks, offering transformative insights into organotitanium chemistry and catalytic cascade design, which will be elaborated upon in subsequent sections.

## 2.6. Hydroxyl radicals-assisted reaction of aldehyde with formaldehyde.

The systematic “carbon growth” with system-produced formaldehyde as the building block is most likely related to the titanium photocatalyzed radical coupling of formaldehyde with methanol<sup>13</sup>. Hydrogen abstraction from the aldehyde side arm of complex **21** induced by hydroxyl radicals will create the corresponding **21 radical** complex, *Figure 7*. This radical couples with formaldehyde creating a **21+CH<sub>2</sub>O** radical intermediate, which isomerizes into an alcohol/aldehyde radical. Via hydrogen atom transfer (HAT) from hydroxyl radicals, a **dehydration** intermediate forms. Subsequent dehydration yields the conjugated double bond seen in complex **22**, showcasing an orderly mechanism for chain extension.

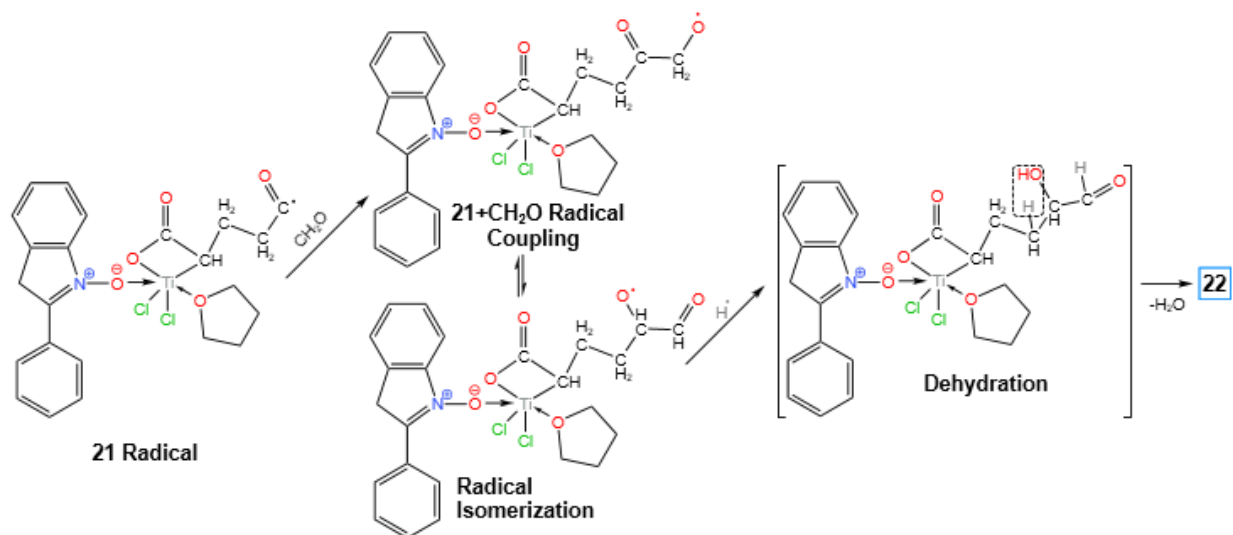


*Figure 7. Mechanism of the photocatalytic coupling of CH<sub>2</sub>O with complex 21 Radical. Isomerization, hydrogenation, and dehydration of transient intermediate to yield complex 22.*

## 2.7 Formation of C<sub>6</sub> to C<sub>9</sub> Oxygenated Hydrocarbons

The hydrolytic separation of complexes **22**, **23**, and **24** yields three primary organic products, identified by MALDI-TOF as MS 128.1728, MS 140, and MS 152, respectively (*Figure 8*). These products correspond to distinct stages of the chain-growth process. Furthermore, these intermediates demonstrate versatility through subsequent transformations, such as acid-catalyzed double-bond hydration, producing a hydrated derivative (MS 176.93), or partial hydrogenation, yielding MS 156. These pathways highlight the catalytic system's capability to generate a diverse array of organic molecules through targeted modifications of the initial products.

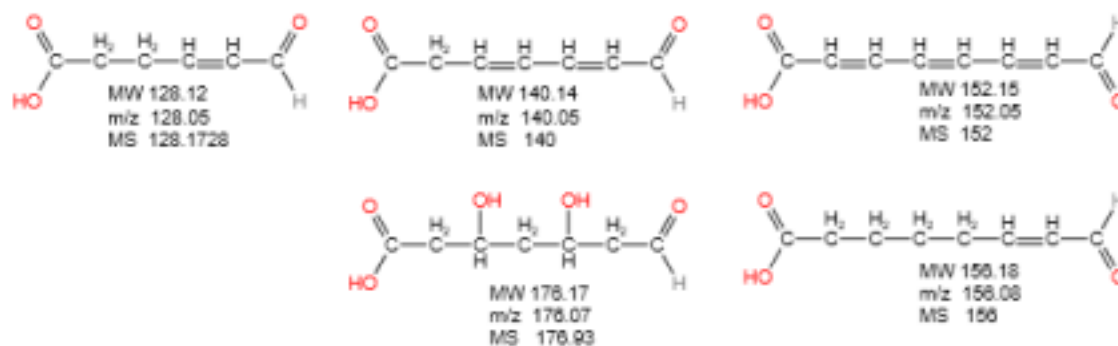


Figure 8.  $\alpha,\omega$ - $C_x$  carboxylic acid-aldehyde unsaturated organics ( $x=6, 7, 8$ ), identified as MS 128.1728, 140, 152, generated by hydrolysis from complexes **22**, **23**, **24**, respectively. Second Row: Corresponding hydrated (MS 176.93) and partially hydrogenated (MS 156) products.

The MALDI-TOF MS data points 199, 216, and 231.939 correspond to three sequentially hydrated  $C_9$  unsaturated organic compounds, as illustrated in Figure 9. These structures are identified as hydrated derivatives of a parent  $C_9$  unsaturated  $\alpha$ -carboxylic acid- $\omega$ -aldehyde compound. However, the exact formation mechanism of this parent compound remains unclear and could not be conclusively determined. This ambiguity underscores a critical gap in understanding the cascade reaction process, necessitating further investigation into the pathways responsible for the generation of these hydrated organic derivatives..

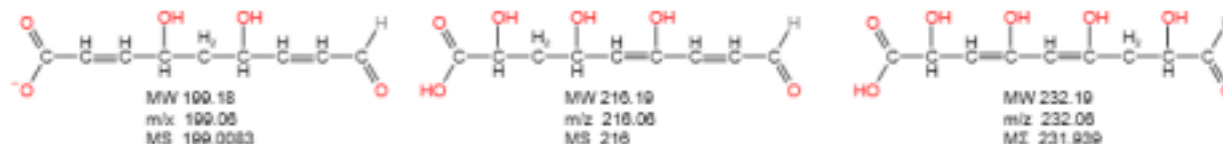


Figure 9. MALDI-TOF identified  $C_9$  oxygenated derivatives.

The organic products corresponding to MS 216 and MS 231.939, both  $C_9$  hydrated unsaturated derivatives, are involved in coupling reactions with a PI radical. In these reactions, the PI radical facilitates the extension or functionalization of the  $C_9$  framework.

## 2.7. Creation of $C_{12}$ to $C_{17}$ and PI coupling products. The essential role of hydroxyl radicals.

The next category of products includes  $C_{12}$  to  $C_{17}$  linear carbon chains, with a notably high concentration of  $C_{16}$  organics. The conspicuous absence of  $C_{10}$  to  $C_{13}$  chains and the apparent upper limit at  $C_{17}$  products are particularly striking. Interestingly, the  $C_{12}$  products in this group originate from an unexpected radical dimerization of MS 128.1728, a  $C_6$  compound mentioned earlier (Figure 8). Hydrogen abstraction from the aldehyde functionality of this compound by hydroxyl radicals generates the corresponding  $C_6$  radical, which subsequently dimerizes to form the  $C_{12}$   $\alpha,\omega$ -diacid (MS 253.909, Figure 10). Similarly, the  $C_{16}$  product (MS 306) arises from a partially hydrogenated  $C_8$  monomer. In this case, aldehyde hydrogen abstraction by hydroxyl radicals produces a  $C_8$  radical that dimerizes to yield an  $\alpha,\omega$ -dicarboxylic acid containing an unsaturated diketone functionality. These findings

provide valuable insights into the radical-driven pathways that govern the formation of higher-order organic products in this system.

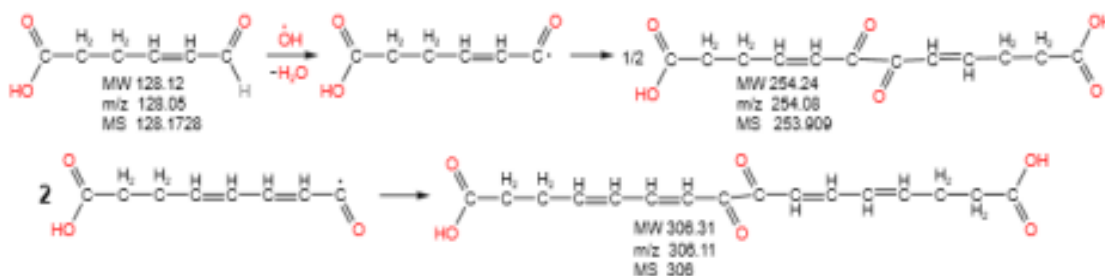


Figure 10. Dimerization of  $C_6$  and  $C_7$  radicals to form  $C_{12}$  and  $C_{14}$  derivatives, respectively.

A  $C_{14}$  dimer originating from the  $C_7$  MS 140 monomer could not be found, but a coupling product between a hydrogenated  $C_6$  and  $C_7$  monomer radical was identified yielding the  $C_{13}$  dicarboxylic acid diketone MS 272, Figure 11.

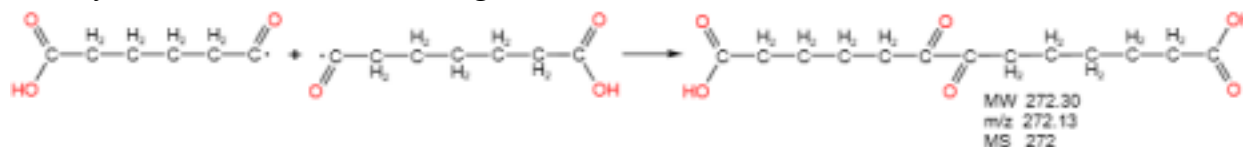


Figure 11. Coupling of  $C_6$  and  $C_7$  radicals yielding the  $C_{13}$  tridecanedioic acid-6,7- diketone MS 272

Coupling of  $C_8$  and  $C_9$  radicals forms the linear  $C_{17}$  heptadecanedioic acid-8,9-diketone MS 328, the longest carbon chain product identified in this system, Figure 12.

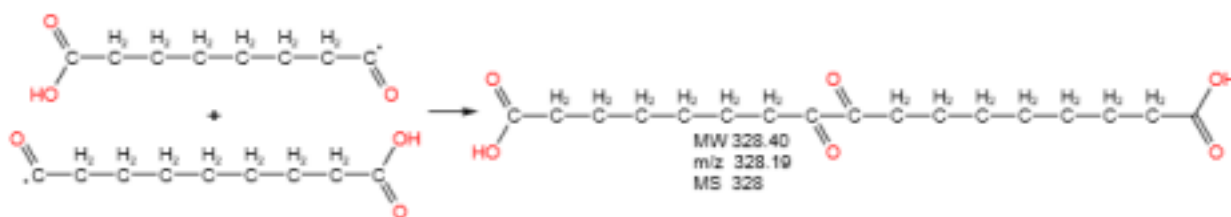


Figure 12.  $C_8$  and  $C_9$  radicals form the  $C_{17}$   $\alpha, \omega$ -heptadecanoic acid-8,9-diketone MS 328.

An unsaturated, partially hydrolyzed  $C_8$   $\alpha, \omega$ -hydroxylic acid keto radical, derived from complex 8, undergoes dimerization to form the  $C_{16}$  unsaturated diacid-diketone-dialcohol (MS 342), as illustrated in Figure 13.

In addition to this product, three closely related  $C_{16}$  organics are observed in the MALDI-TOF spectrum:

1. A derivative with an additional hydroxyl group (MS 358).
2. A compound featuring exclusively single carbon-carbon bonds and one extra hydroxyl group (MS 378).
3. A fully hydrogenated version of the MS 378 compound, where the two ketone groups are reduced to hydroxyl groups, resulting in MS 382.

These findings highlight the diversity of  $C_{16}$  compounds generated within this system, reflecting the intricate interplay of radical dimerization, partial hydrolysis, and hydrogenation processes.

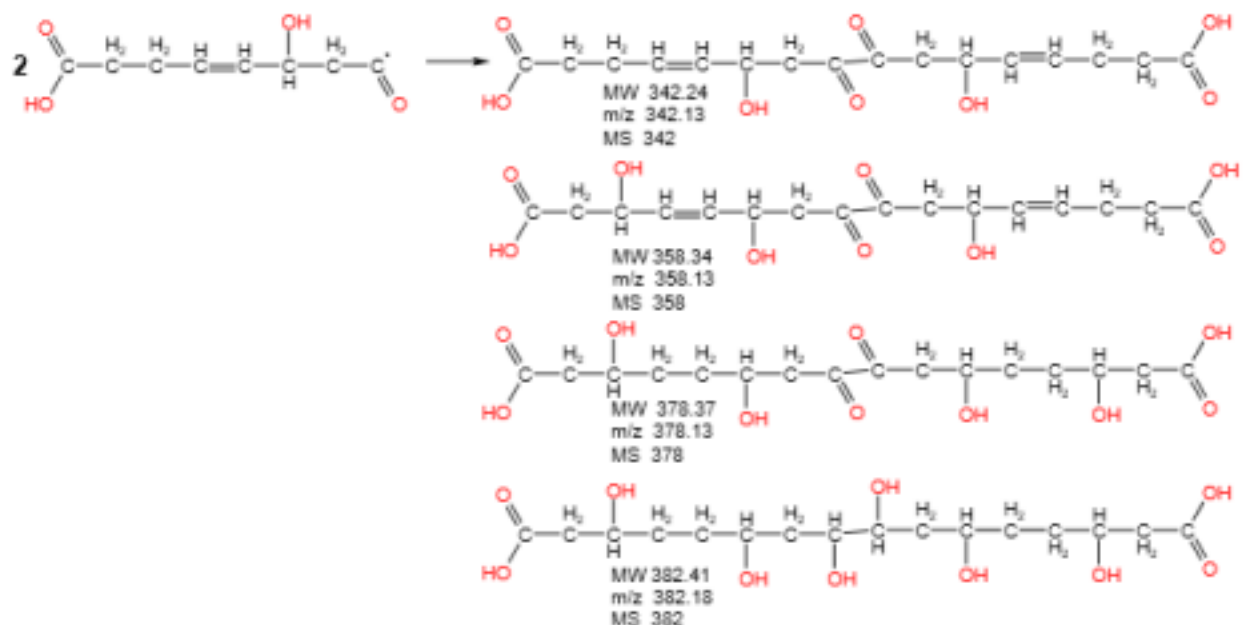


Figure 13. Formation of linear  $C_{16}$  oxygenated compounds, derivatives of the  $\alpha,\omega$ -hexadecanedioic acid, by dimerization of  $C_8$  carbonyl radicals originating from complex **24**.

## 2.8 Coupling of $C_9$ products with 2-Phenyl Indole Radicals

A third class of compounds produced by our photocatalytic system arises from radical-induced couplings between  $C_9$  oxygenated keto radicals and PI radicals, yielding MS 407 and MS 423 (Figure 14). The formation of these products aligns with the expected availability of PI radicals, as evidenced by the previously described radical oligomerization of PI during system operation<sup>1</sup>.

This class also includes two additional products, MS 457.947 and MS 474.12, which result from the coupling of related  $C_9$  radicals with 5-position chlorinated PI radicals (Figure 15). Notably, the coupling process appears to favor  $C_9$  acid/alcohol unsaturated chain keto radicals over shorter counterparts ( $C_6$ – $C_8$ ). This preference may be attributed to the longer half-life of  $C_9$  radicals within the system.

Table 1 organizes all products identified in the photocatalytic cycle, listed by their appearance in the MALDI-TOF MS spectrum (Figure 5) along with their relative intensities, extracted using methylene chloride. Several noteworthy items are:

**Nu. 6:** PI

**Nu. 19:** Hydrogenated PI dimer.

**Nu. 24 and Nu. 25:** Unassigned products.

Among the higher molecular weight products:

**Nu. 26:** PI trimer.

**Nu. 28:** PI tetramer.

**Nu. 30:** Hydrogenated PI pentamer.

**Nu. 31:** Hydrogenated PI hexamer.

Additionally, Nu. 27 and Nu. 29 remain unidentified, representing potential coupling products. These observations underscore the complexity and richness of the photocatalytic system in generating diverse organic products through a combination of radical coupling, oligomerization, hydrolysis, and hydrogenation processes.

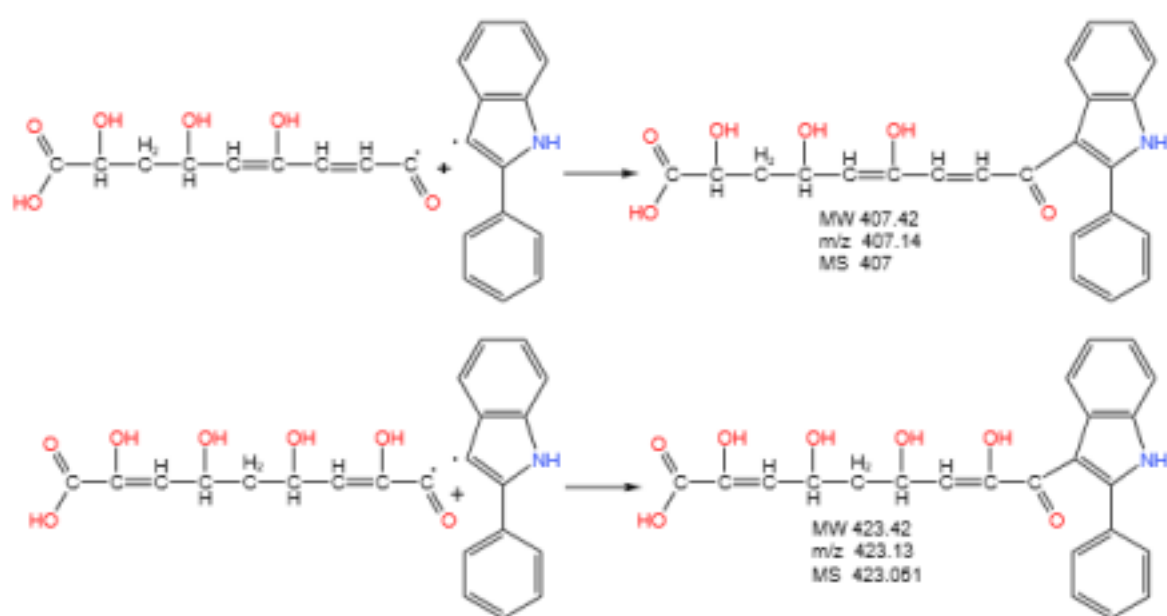


Figure 14. . Reaction of  $C_9$  radicals with PI radicals.

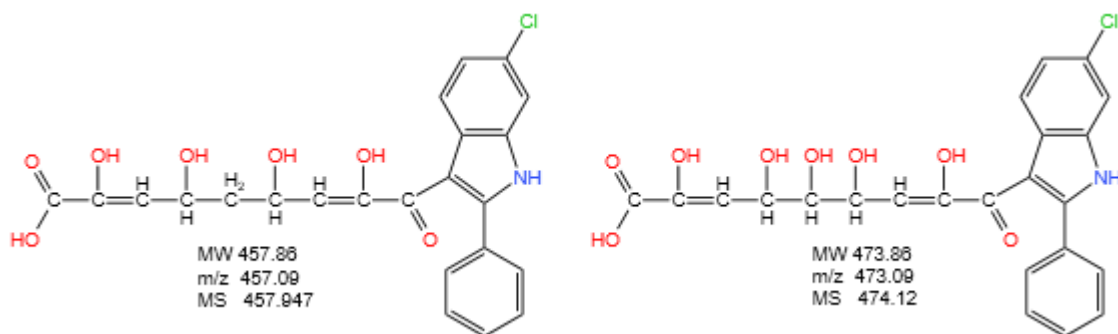


Figure 15. Coupling products of  $C_9$  radicals with chlorinated PI.

### 3. Experimental

(PI)<sub>2</sub>TiCl<sub>4</sub> was prepared following a published procedure.<sup>1</sup>

MALDI-TOF MS Spectra: Recorded with a Bruker instrument run with Daltonics autoflexR maX Analysis software. Solid samples chosen for analysis were suspended in CH<sub>2</sub>Cl<sub>2</sub>.

## 4. Conclusion

The production of C<sub>6</sub>-C<sub>17</sub> oxygenated hydrocarbons from organotitanium compounds as described in this study represents a significant advancement in the field of organotitanium chemistry and artificial photosynthesis. Our work demonstrates that titanium-based catalysts, when properly tuned, can facilitate the formation of valuable, longer-chain oxygenated hydrocarbons under mild conditions. This method leverages the unique properties of titanium, particularly its ability to form stable intermediates while maintaining high reactivity, which has allowed for a cleaner and more direct pathway from simple starting materials, such as atmospheric CO<sub>2</sub> and water.

This research highlights the potential of organotitanium chemistry to bridge the gap between laboratory-scale artificial photosynthesis processes and practical applications in chemical synthesis and renewable energy. The capability to directly produce C<sub>6</sub>-C<sub>17</sub> hydrocarbons, which are critical intermediates in the chemical industry, positions this method as a promising alternative to conventional petrochemical routes. By generating these compounds from sustainable sources, we move one step closer to replacing fossil fuel-dependent methods with environmentally friendly and carbon-neutral processes.

Additionally, the ability to control the chain length and functionalization of these oxygenated hydrocarbons provides a versatile platform for synthesizing a range of chemicals, including biofuels, lubricants, and specialty chemicals. Future work will focus on further optimizing the catalyst system to enhance selectivity, yield, and overall efficiency. Moreover, improving our understanding of the reaction mechanisms at play will help in scaling up the process for industrial application, ensuring that it is not only sustainable but also economically viable.

In conclusion, this study opens new avenues for the use of organotitanium compounds in the generation of oxygenated hydrocarbons, contributing to the ongoing efforts to develop artificial photosynthesis technologies. The implications of this work extend beyond synthetic chemistry, offering a pathway to reduce carbon emissions and create more sustainable industrial processes. Future research will aim to address the challenges of scalability, economic feasibility, and environmental impact, with the ultimate goal of integrating this system into broader renewable energy frameworks.

## References

1. Paraskevas M.; Arzoumanidis G.G. Artificial Photosynthesis: Visible Light-Activated TiOCl<sub>2</sub>/ 2-Phenyl Indole Complexes for Atmospheric CO<sub>2</sub> and H<sub>2</sub>O Capture and Long Chain Organic Products Generation. *Fine Chemical Engineering* **2024**, *5*, 369-396, Open Access.
2. Godemann, C.; Dura, L.; Hollmann, D.; Grabow, K.; Bentrapp, U.; Jiao, H.; Schulz, A.; Brückner, A.; and Beweries, Y. Highly selective visible light-induced Ti-O bond splitting in an ansa-titanocene dihydroxido complex. *Chem. Commun.* **2015**, *51(14)*, 3065-3068.
3. Godemann, C.; Hollmann, D.; Kessler, M.; Jiao, H.; Spannenberg, A.; Brückner, A.; and Beweries, T. A Model of a Closed Cycle of Water Splitting Using *ansa*-Titanocene (III/IV) Triflate Complexes. *J. Am. Chem. Soc.* **2015**, *137*, 16187-16195



4. Kitano, M.; Tsujimaru, K.; Anpo, M. Hydrogen production using highly active titanium oxide-based photocatalysts. *Top Catal.* **2008**, *49*(1), 4-17.
5. Eidsvag, H.; Bentouba, S.; Vajeeston, P.; Yohi, S.; Velauthapillai, D. TiO<sub>2</sub> as a photocatalyst for water splitting - An experimental and theoretical review. *Molecules* **2021**, *26*(7), 1687-1727.
6. Nakajima, T.; Tamaki, Y.; Ueno, K.; Kato, E.; Noshikawa, T.; Ohkubo, K.; Yamazaki, Y.; Morimoto, T.; Ishitani, O. Photocatalytic reduction of low concentration of CO<sub>2</sub>. *J. Am. Chem. Soc.* **2016**, *138*(42), 13818-13821.
7. Nosaka, Y.; Nosaka, A. Understanding Hydroxyl Radical(.OH) Generation Processes in Photocatalysis. *ACS Energy Letters* **2016**, *1*, 2, 356-359.
8. G. Arzoumanidis, G. . Organotitanium Click Chemistry. *Fine Chemical Engineering* **2023**, *4*, 147-174, Open Access
9. Dauth, A.; Love J. A. Reactivity by Design--Metallaoxetanes as Centerpieces in Reaction Development. *Chem. Rev.* **2011**, *111*, 2010-2042.
10. Bailey, G. A.; Fogg, D. E. Confronting neutrality: Maximizing success in the analysis of transition-metal catalysts by MALDI mass spectrometry. *ACS Catal.* **2016**, *6*, 4962-4971.
11. Dopke, N. C.; Treichel, P. M.; Vestling, M. M. Matrix-assisted laser desorption/ionization time-of-flight mass spectroscopy (MALDI-TOF MS) of Rhenium(III) halides: A characterization tool for metal atom clusters. *Inorg. Chem.* **1998**, *37*(6), 1272-1277.
12. Wang, T.-H.; Navarrete-Lopez, A. M.; Li, S.; Dixon, D. A.; Gole, J. L. Hydrolysis of TiCl<sub>4</sub>: Initial steps in the production of TiO<sub>2</sub>. *J. Phys. Chem. A* **2010**, *114*(28), 7561-7570.
13. Fan, Y.; Bao, J.; Shi, L.; Li, S.; Lu, Y.; Liu, H.; Wang, H.; Zhong, L.; Sun, Y. Photocatalytic coupling of methanol and formaldehyde into ethylene glycol with high atomic efficiency. *Catal. Lett.* **2018**, *148*, 2274-2282.

## Author contributions

This manuscript was written by GGA with contributions from both authors. GGA suggested this study and interpreted the experimental data. MP performed the experimental work and chose the analytical tools.

## Conflict of interest

The authors declare no competing financial interest

